pH-Induced Vesicle-to-Micelle Transition in Amphiphilic Diblock Copolymer: Investigation by Energy Transfer between in Situ Formed Polymer Embedded Gold Nanoparticles and Fluoresce...

ARTICLE *in* LANGMUIR · DECEMBER 2014

Impact Factor: 4.46 · DOI: 10.1021/la504165e · Source: PubMed

4 AUTHORS, INCLUDING:

Chiranjit Maiti
IIT Kharagpur
6 PUBLICATIONS **12** CITATIONS
SEE PROFILE

Saikat Maiti
IIT Kharagpur
5 PUBLICATIONS **12** CITATIONS
SEE PROFILE

Langmuir

Article

pubs.acs.org/Langmuir

pH-Induced Vesicle-to-Micelle Transition in Amphiphilic Diblock Copolymer: Investigation by Energy Transfer between *in Situ* Formed Polymer Embedded Gold Nanoparticles and Fluorescent Dye

Chiranjit Maiti, Rakesh Banerjee, Saikat Maiti, and Dibakar Dhara*

Department of Chemistry, Indian Institute of Technology Kharagpur, Kharagpur, West Bengal 721302, India

Supporting Information

ABSTRACT: The ability to regulate the formation of nanostructures through self-assembly of amphiphilic block copolymers is of immense significance in the field of biology and medicine. In this work, a new block copolymer synthesized by using reversible addition−fragmentation chain transfer (RAFT) polymerization technique from poly(ethylene glycol) monomethyl ether acrylate (PEGMA) and Boc-L-tryptophan acryloyloxyethyl ester (Boc-L-trp-HEA) was found to spontaneously form pH-responsive water-soluble nanostructures after removal of the Boc group. While polymer vesicles or polymerosomes were formed at physiological pH, the micelles were formed at acidic pH (< 5.2), and this facilitated a pH-induced reversible vesicle-to-micelle transition. Formation of these nanostructures was confirmed by different characterization techniques, viz. transmission electron microscopy, dynamic light scattering, and steady-state fluorescence measurements. Further, these vesicles were successfully utilized to reduce $HAuCl_4$ and stabilize the resulting gold nanoparticles (AuNPs). These AuNPs, confined within the hydrophobic shell of the vesicles, could participate in energy transfer process with fluorescent dye molecules encapsulated in the core of the vesicles, thus forming a nanometal surface energy transfer (NSET) pair. Subsequently, following the efficiency of energy transfer between this pair, it was possible to monitor the process of transition from vesicles to micelles. Thus, in this work, we have successfully demonstrated that NSET can be used to follow the transition between nanostructures formed by amphiphilic block copolymers.

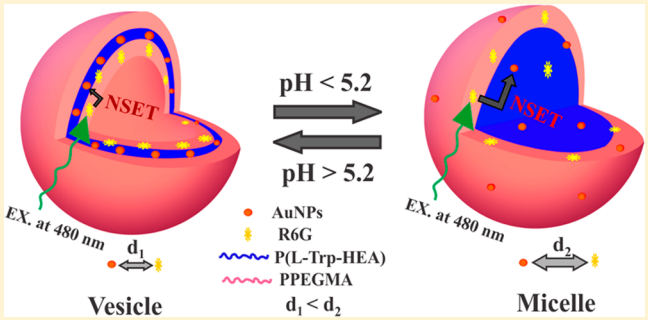

INTRODUCTION

Nanostructures from block copolymers, particularly from amphiphilic block copolymers, have aroused great interest among researchers because of their potential use in cosmetics, catalysis, electronics, and drug delivery.[1−4] The self-assembly of amphiphilic block copolymer molecules that leads to the formation of the nanostructures in aqueous systems depends on the hydrophobic−hydrophilic balance of the block copolymers. Stimuli responsive amphiphilic block polymers are even more attractive owing to their ability to generate versatile nanostructured assemblies such as micelles[5,6] and vesicles[2,7,8] and hence have the potential to be effective as stimuli sensitive delivery vehicles for therapeutics.[1,2,8,9] A great deal of effort has been focused on the synthesis of stimuli responsive block copolymers that are capable of undergoing conformational changes or phase transitions in solution with change in external stimuli like pH, temperature, and ionic strength.[7,10,11]

Most of the methods for preparation of vesicles from amphiphilic molecules typically involve the use of an organic solvent such as tetrahydrofuran, *N*,*N*-dimethylformamide (DMF), or dioxane.[12−14] This method, however, is not preferred because of the toxicity associated with the organic solvents. Elaborate purification methods like dialysis are generally required to remove the organic solvent, making the process cost-ineffective. Furthermore, dialysis rate and solvent dependence on self-assembly are difficult to control. In this regard, water-soluble block copolymers that spontaneously form vesicles are highly desirable. Additionally, polymer vesicles or polymersomes made of amphiphilic copolymers have an aqueous core separated from the outside by a hydrophobic membrane with both external and internal surfaces formed by hydrophilic polymer.[12,15−17] Thus, vesicles can encapsulate both hydrophobic and hydrophilic molecules. If a vesicle can be transitioned to micelle *in situ* by a stimulus, then the hydrophilic molecules can be selectively released from the vesicles' hydrophilic core.[18−20] In the present work, we have synthesized a new diblock copolymer by using the reversible addition−fragmentation chain transfer (RAFT) polymerization technique from highly biocompatible monomers poly(ethylene glycol) monomethyl ether acrylate (PEGMA) and Boc-L-tryptophan acryloyloxyethyl ester (Boc-L-trp-HEA). The Boc group deprotected block copolymer spontaneously forms vesicles in aqueous solution at physiological pH, which can be reversibly transitioned to micelles by changing the pH of the

Received: June 30, 2014
Revised: December 12, 2014
Published: December 15, 2014

DOI: 10.1021/la504165e
Langmuir 2015, 31, 32−41

Scheme 1. Schematic Representation of Synthesis of Diblock Copolymers (Poly(L-Trp-HEA)-*b*-poly(PEGMA)) Using the RAFT Polymerization Technique

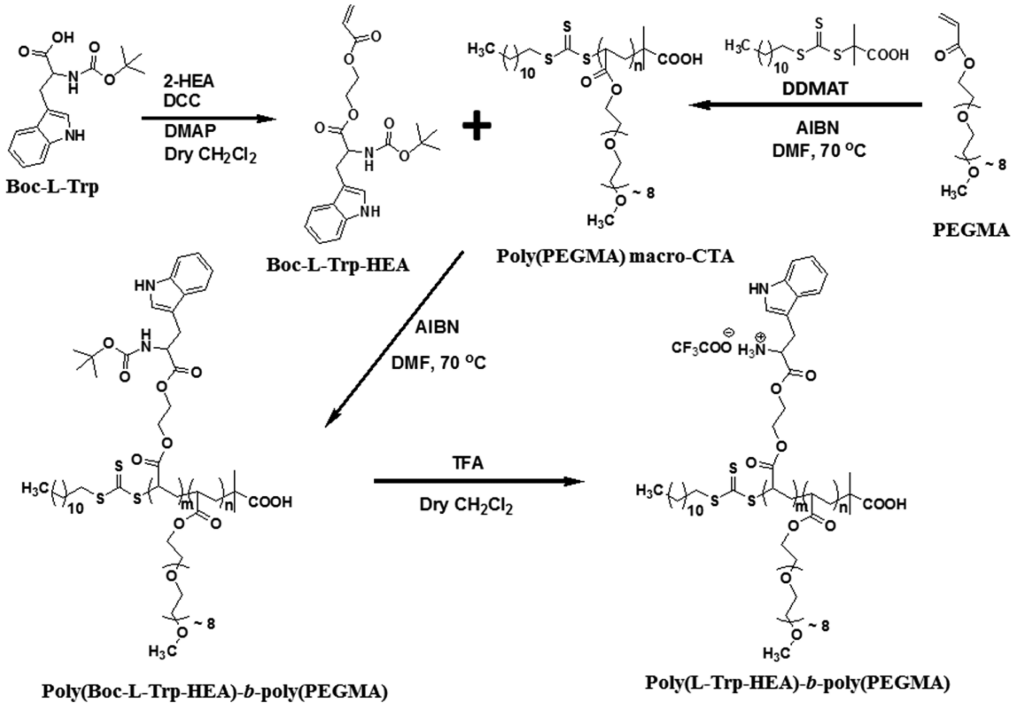

medium. This pH-induced vesicle-to-micelle transition below a critical transition pH resulted in selective triggered release of encapsulated hydrophilic guest molecules over hydrophobic ones.

Noble metal nanoparticles, especially gold nanoparticles (AuNPs), have always been in great interest for biological applications.[21] Bioconjugates of AuNPs, for example, DNA–AuNPs bioconjugates, can be utilize for targeted drug delivery, CT imaging, and therapy.[22,23] *In situ* synthesis of AuNPs into the drug loaded polymer nanostructures could be very useful for nanotechnological and biological applications. For example, polymer vesicles embedded AuNPs could impart detectability to the polymer vesicles. In this work, we have also investigated the possibility of formation of stable polymer embedded AuNPs by the polymer vesicles from the present block copolymer. We show that the polymer vesicles, formed spontaneously from the synthesized block copolymer, were able to reduce $HAuCl_4$ and stabilize the resulting AuNPs.

Recently, Chen et al.[24] investigated nanometal surface energy transfer (NSET) as an optical ruler for the measurement of binding site distances on live cell surfaces. Another motivation of the present study is to establish a new type of plasmonic nanohybrid[25] with AuNPs and fluorescent dyes, which could enable the employment of plasmon coupled optical properties such as NSET in sensing, nanophotonics, and biological applications. In this study, we have also shown that AuNPs confined to the vesicles could participate in energy transfer process with a hydrophilic fluorescent dye which was encapsulated in the vesicle and form a NSET pair. By following the efficiency of energy transfer between this pair, it was possible to monitor the process of transition from vesicles to micelle. Although the energy transfer technique has been used to probe polymeric aggregates in a few occasions,[26−28] to the best of our knowledge, this is the first report where pH-induced vesicle to micelle transition of an amphiphilic block copolymer could be probed by such an elegant spectroscopic technique.

EXPERIMENTAL SECTION

Materials. Poly(ethylene glycol) monomethyl ether acrylate (PEGMA, MW 480), 4-(dimethylamino)pyridine (DMAP), dicyclohexylcarbodiimide (DCC), 2-hydroxyethyl acrylate (HEA), and gold(III) chloride trihydrate ($HAuCl_4{\cdot}3H_2O$) were purchased from Sigma-Aldrich and used without further purification. *S*-1-Dodecyl-*S*′-(α,α′-dimethyl-α″-acetic acid) trithiocarbonate (DDMAT) was synthesized according to the literature reported procedure.[10,29] Boc-L-tryptophan (Boc-L-Trp) and trifluoroacetic acid (TFA) were purchased from Sisco Research Laboratories Pvt. Ltd., India, and used as received. 2,2′-Azobisisobutyronitrile (AIBN, Sigma-Aldrich) was recrystallized twice from methanol before use. Procedures for synthesis of tryptophan containing monomer (Boc-L-Trp-HEA) and poly(PEGMA)-based macro-chain-transfer agent (CTA) (Scheme 1) are provided in the Supporting Information. Rhodamine 6G (R6G) and Nile Red (laser grade, Exciton) were used as received. Milli-Q water was used in all the experiments.

Synthesis of Poly(Boc-L-Trp-HEA)-b-poly(PEGMA) Diblock Copolymer (Scheme 1). For the synthesis of block copolymer (Boc-L-Trp-HEA) (0.6 g, 1.5 mmol) and poly(PEGMA) macro-CTA (0.7 g, 0.03 mmol) were added along with dry DMF (2.0 mL) to a 10 mL septa-sealed single-necked round-bottomed flask containing a magnetic stir bar. AIBN (1.5 mg, 0.009 mmol) dissolved in dry DMF (0.1 mL) was then added to it. The reaction content was placed in a preheated oil bath at 70 °C after purging with N_2 gas for 30 min. The reaction was quenched after 24 h by cooling the reaction flask in a liquid nitrogen bath. The product was then diluted by small aliquots of methanol and dialyzed against methanol using cellulose membranes (MW cutoff value of 12 kDa) for 2 days with frequent change of methanol (three times in 1 day), and the product was obtained by evaporating methanol in rotary evaporator and finally dried under high vacuum. The composition and number-average molecular weight of the synthesized polymers were determined by the utilization of ^{1}H NMR spectroscopy. ^{1}H NMR spectra are provided in the Supporting Information (Figure S5).

DOI: 10.1021/la504165e
Langmuir 2015, 31, 32−41

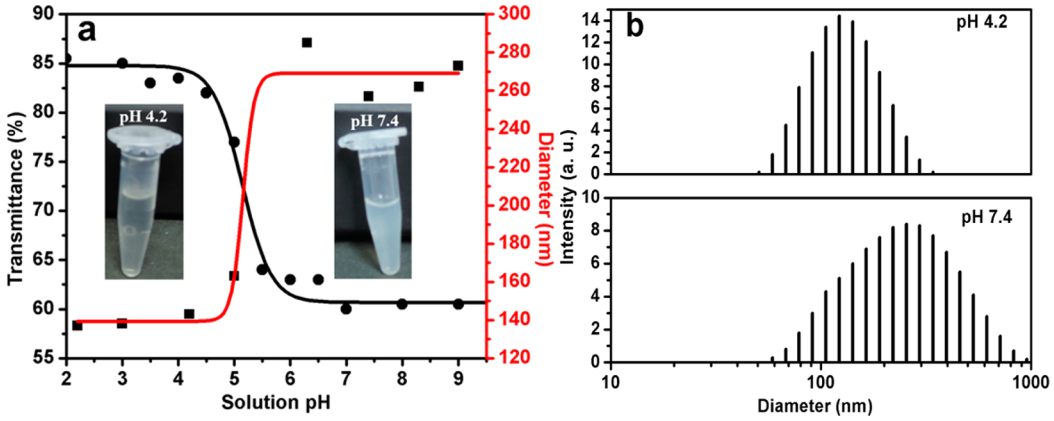

Figure 1. (a) Plot of transmittance (%) at 500 nm and hydrodynamic diameter of 0.2 mM poly(L-Trp-HEA)-*b*-poly(PEGMA) copolymer solution with increasing solution pH (inset: photo of the block copolymer solution at two representative pH). (b) Size distribution profiles of the poly(L-Trp-HEA)-*b*-poly(PEGMA) obtained from dynamic light scattering measurement at two different solution pH: below and above the transition pH.

Boc Group Deprotection (Scheme 1). 0.6 g of the above block copolymer was dissolved in 5.0 mL of dry CH_2Cl_2 in a 25 mL double-necked round-bottomed flask, and trifluoroacetic acid (TFA) (0.5 mL) was added dropwise using a syringe. The solution was kept at room temperature under a nitrogen atmosphere with continuous stirring for 24 h. After that TFA was removed by azeotropic distillation with toluene, and finally the product was purified by dialysis against distilled water using cellulose membranes (MW cutoff value of 12 kDa) for 3 days with frequent change of water (four times in 1 day). The purified copolymer solution was freeze-dried and analyzed by ^{1}H NMR spectroscopy for its final composition (for ^{1}H NMR spectra, see the Supporting Information, Figure S6).

Gold Nanoparticle-Embedded Vesicle Preparation. Polymer vesicle solution (0.2 mM) prepared using the poly(L-Trp-HEA)-*b*-poly(PEGMA) copolymer in 10 mM phosphate buffer at pH 7.4 is taken in a vial containing a magnetic stirrer and stirred at 450 rpm. After 5 min, $HAuCl_4$ solution in phosphate buffer was added dropwise at 25 °C temperature to give a L-Trp-HEA to Au ratio of 10 to 1. The mixed solution was allowed to stir overnight; within this time the color of the solution changed from light yellow to red pink which indicated formation of stable AuNPs.

Instrumentation and Methods. Instruments and methods used for recording NMR, GPC, UV−vis, steady-state, and time-resolved fluorescence spectra, measuring turbidity, structural characterization (TEM, DLS), determination of critical aggregation concentration (CAC) of the block copolymer, encapsulation of Rhodamine 6G (R6G) in the vesicular assemblies, calculation of fluorescence quantum yield, and NSET parameters are provided in the Supporting Information.

RESULTS AND DISCUSSION

Synthesis of the Diblock Copolymer. Well-defined block copolymer was synthesized from acrylate monomers having L-tryptophan moiety (Boc-L-Trp-HEA) and poly(ethylene glycol) monomethyl ether acrylate (PEGMA) using the RAFT technique, which is an efficient tool for controlled polymerization. In the first step, poly(PEGMA) macro-CTA was synthesized by polymerization of PEGMA by using DDMAT as chain transfer agent. End-group analysis by ^{1}H NMR spectroscopy was utilized for the determination of composition and number-average molecular weight of the synthesized polymers because this method provides absolute and more reliable data for quantification.[30] The molecular weight of the poly(PEGMA) macro-CTA was quantified by integration of the three protons of the terminal methyl group of dodecyl unit of DDMAT (at 0.85 ppm) with respect to three protons of methyl group at 3.35 ppm of PEGMA repeat units (for ^{1}H NMR spectra, please see the Supporting Information, Figure S1). The poly(PEGMA) macro-CTA was found to consist of 50 PEGMA units that correspond to a M_n of ∼24 400 g mol^{-1}. Gel permeation chromatography (GPC) analysis of the macro-CTA (see Supporting Information, Figure S2) revealed monomodal distributions with a M_n value of ∼22 500 g mol^{-1} and polydispersity index (PDI) 1.07, indicating a good control over the polymerization.

In the next step, another acrylate monomers containing amino acid (L-tryptophan) moiety (Boc-L-Trp-HEA) was synthesized by a coupling reaction of Boc protected L-tryptophan with 2-hydroxyethyl acrylate (HEA) (see the Supporting Information for ^{1}H NMR and ^{13}C NMR spectra, Figures S3 and S4). After successful synthesis of Boc-L-Trp-HEA, poly(PEGMA) macro-CTA was employed for the synthesis of block copolymer with desired number of Boc-L-Trp-HEA repeat units. The composition of the block copolymer was determined by integration of the intensities of the one aromatic proton at 7.49 ppm in the poly(Boc-L-Trp-HEA) block and comparing with the intensity of three protons of methyl group in the poly(PEGMA) block (at 3.37 ppm) (Figure S5, Supporting Information). Boc group removal from poly(Boc-L-Trp-HEA)-*b*-poly(PEGMA) using TFA yields desired block copolymer with free primary amine groups (Figure S6, Supporting Information). The molecular weight of the second block, poly(L-Trp-HEA), was determined from the copolymer composition using ^{1}H NMR spectroscopy. The molar ratio of PEGMA/L-Trp-HEA was found to be 50:47, and the molecular weight of the block copolymer was calculated to be ∼38 600 g mol^{-1}. Furthermore, M_n value obtained from GPC analysis was ∼35 300 g mol^{-1}, which is very close to the data obtained from ^{1}H NMR spectroscopy and the molecular weight was narrowly distributed as indicated by the low PDI of 1.17 (Figure S2, Supporting Information).

pH-Responsive Solution Properties of Diblock Copolymers. The free primary amine groups present in the polymer chains can be protonated and deprotonated reversibly by changing the pH of the polymer solution.[31] To study pH-dependent solution properties of poly(L-Trp-HEA)-*b*-poly(PEGMA) copolymer, we monitored the effect of pH on the transmittance of a 0.2 mM aqueous buffer solutions of the block copolymer at 500 nm (Figure 1a). The transmittance values were found to be almost invariant up to pH 4 and then started decreasing sharply at higher pH. At lower pH values free

DOI: 10.1021/la504165e
Langmuir 2015, 31, 32−41

amine groups are in a completely protonated state, and the polymers are readily soluble. Above this pH, the majority of the protonated amino groups were converted to free primary amine groups leading to sharp decrease of transmittance value. The transition pH of poly(L-Trp-HEA) block in aqueous solution of poly(L-Trp-HEA)-*b*-poly(PEGMA) copolymer was found to be close to 5.2, where ~50% drop in transmittance was observed (Figure 1a). The decrease in the solubility of the block copolymer is due to the increased hydrophobicity of poly(L-Trp-HEA) block in the copolymer with increase in the solution pH as a result of deprotonation of primary amine group. To check the solubility, we kept the polymer solution at pH 7.4 for over 2 weeks at room temperature. No precipitation was observed, indicating the soluble nature of the block copolymer at that pH, which hinted at the formation of stable self-assembled nanostructures.

To understand the influence of pH on self-assembly of this block copolymer, we carried out dynamic light scattering (DLS) experiment of 0.2 mM aqueous polymer solution with increasing solution pH (Figure 1a). The results obtained from DLS measurements corroborated well with the results of transmittance measurements. At lower pH values, the particle size was found to be almost invariant of pH, but above the transition pH value (pH = 5.2) significant increase of particle size was observed. DLS and transmittance measurements on decreasing the solution pH in the reverse direction showed the reversible nature of this pH-induced change of particle size and solubility. Figure 1b represent the distribution of hydrodynamic diameter of the block copolymer at two representative pH: one below (pH 4.2) and one above (pH 7.4) the transition pH. DLS study revealed an average hydrodynamic diameter in the range of 143 nm for the copolymer at pH 4.2, whereas by increasing the solution pH to 7.4 the average hydrodynamic diameter value increased to 262 nm. Thus, from DLS data, it was clear that at even below pH 5.2 the copolymer did not exist as unimer, and self-assembled nanostructures were indeed present in the solution. This was possible only if the polymer concentration was above its critical aggregation concentration, CAC, the concentration above which it forms self-assembled aggregates in water.[32] We have estimated CAC of this block copolymer at pH 7.4 and 4.2 using Nile Red as fluorescent probe.[33] It is known that Nile Red on its own has negligible solubility in water, and thus an aqueous solution of Nile Red shows very weak fluorescence with emission maxima at 661 nm (λ_{ex} = 550 nm). Figure 2 shows the plot of Nile Red fluorescence intensity at the emission maxima at pH 7.4 and 4.2 versus the log of polymer concentration. Nile Red emission intensity changed in a nonlinear fashion as a function of the polymer concentration. At low concentration range of the polymer, both emission intensity and the emission maxima were unchanged, which indicates that Nile Red remained in an environment similar to pure water. Above a specific concentration of the block copolymer, the emission intensity of Nile Red increased considerably with simultaneous blue-shifting of the emission maxima. This indicated that the dye molecules were encapsulated in the hydrophobic regions that were formed owing to self-assembly of the block copolymer molecules. An inflection point was achieved from the plot of Nile Red emission intensity versus the log of polymer concentration, and the concentration corresponding to that inflection point was considered as the CAC of the block polymer. For the block copolymer used in the present study, the value of the CAC was found to be ~0.003 mM or 0.11 mg mL^{-1} (Figure 2) at pH 7.4, and at pH 4.2 this value increased to 0.005 mM (0.19 mg mL^{-1}) which is comparable to the CAC values reported in the literature for similar copolymers.[10,34,35] This change of CAC value of poly(L-Trp-HEA)-*b*-poly(PEGMA) copolymer with respect to solution pH hinted at a stimuli (pH) responsive change of aggregation property. At pH 7.4 the amino groups are deprotonated, making the poly(L-Trp-HEA) block more hydrophobic than at pH 4.2. This brings down the CAC of the block copolymer at pH 7.4 in comparison to the CAC value at pH 4.2. It is noteworthy that a significant difference in the hydrodynamic size of the block copolymer nanostructures was observed at pH 4.2 and pH 7.4 (Figure 1b). To determine the nature of the self-assembled nanostructures at the two pH, transmission electron microscopy (TEM) study was carried out with and without using cryofixation. TEM studies revealed (Figure 3a,c) that at pH 7.4 poly(L-Trp-HEA)-*b*-poly(PEGMA) copolymer formed spherical aggregates (diameter in the range of ~300 ± 50 nm) with a darker thin wall and a hollow interior, symptomatic of vesicular assembly. While lowering the solution pH, the same polymer produced dark, near-spherical particles of diameter ~130 ± 20 nm, suggesting micelle-like aggregates. Dimensions of the particles found from TEM images corroborated well with the average hydrodynamic diameter obtained from DLS measurement, as mentioned earlier. Below the transition pH, the amino groups of the poly(L-Trp-HEA)-*b*-poly(PEGMA) copolymer became protonated, which decreased the hydrophobicity of the poly(L-Trp-HEA) block. Because of this protonation and reduced hydrophobicity, the poly(L-Trp-HEA) block experienced electrostatic repulsion and formed relatively less compact miceller aggregates. This probably explains the observed hydrodynamic diameter of the micelles that is higher than that expected from the Gaussian coil structure of the present polymer. Large micelles (D_H ~ 200 nm) formed by the self-assembly of the diblock copolymer molecules having similar or lower molecular weights than used here have also been reported earlier by other researchers.[36−38] It is worth mentioning that the change in the hydrodynamic size and nature of nanostructure formation can be achieved reversibly by simply changing the pH of the solution.

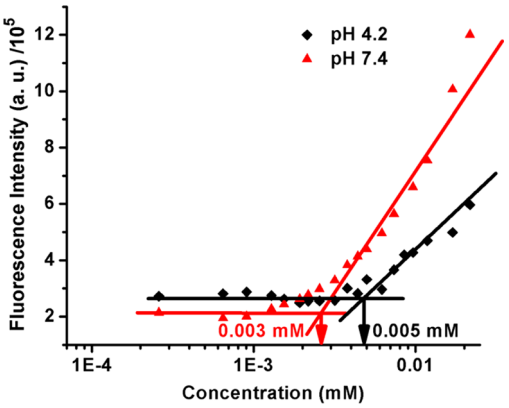

Figure 2. Plot of Nile Red fluorescence intensity (λ_{ex} = 550 nm) at the emission maxima versus the log of polymer concentration to determine the critical aggregation concentration (CAC) at two representative solution pH: 7.4 and 4.2.

Guest Molecules (Nile Red and R6G) Encapsulation and Release. We examined the effect of pH-induced vesicle-to-micelle transition on the fate of guest molecules encapsulation and release.[18,39] To investigate this, we utilized R6G and Nile

DOI: 10.1021/la504165e
Langmuir 2015, 31, 32−41

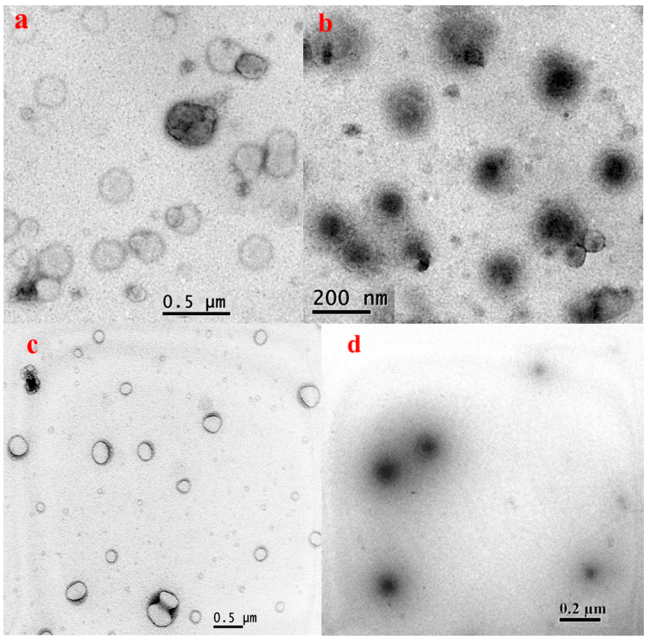

Figure 3. TEM image of (a) the vesicles obtained from aqueous solution of poly(L-Trp-HEA)-*b*-poly(PEGMA) at 7.4 solution pH and (b) the micelles obtained by lowering pH the same solution from 7.4 to 4.2; (c) and (d) show the cryo-TEM images of the vesicles and the micelles, respectively.

Red as a hydrophilic and hydrophobic dye, respectively. R6G was incorporated into the polymer vesicles (polymerosomes) by sonication of the aqueous solution of poly(L-Trp-HEA)-*b*-poly(PEGMA) at pH 7.4 for 15 min. This was followed by extensive dialysis to ensure of the complete removal of the nonencapsulated or free dye molecules. Figure S7a (Supporting Information) shows the absorption spectra of R6G encapsulated into the polymer aggregates and in polymer-free aqueous buffer solution at pH 7.4. Aqueous solution of R6G at pH 7.4 showed absorption maxima at 527[40] and 532 nm in the absence and presence of polymer, respectively. This red-shift of 5 nm in the absorption maxima indicates efficient loading of R6G into the polymer nanostructures. We have determined the concentration of R6G molecules encapsulated into the vesicles using UV−vis absorption, and it was found to be 8.6 μM. Concentration-normalized fluorescence spectra of R6G encapsulated into the polymer nanostructures and in polymer-free aqueous solution at pH 7.4 are depicted in Figure S7b (Supporting Information). A huge (~50%) reduction of the emission intensity at 557 nm was observed for the dialyzed solution containing R6G compared to that of absorbance matched aqueous R6G solution in the absence of the block polymer at same solution pH (7.4). This observed quenching of fluorescence may be attributed to the confinement of R6G into the water-filled interior of the vesicles. Similar self-quenching nature of the hydrophilic dye molecules due to confinement has been reported earlier in vesicular assemblies.[10,41,42]

On the other hand, it is also known that tryptophan can act as an electron donor in photoinduced electron transfer (PET) reactions with R6G dye molecules which may also contribute to the quenching of R6G fluorescence in the present polymeric system containing a tryptophan moiety.[43] To avoid confusion, we have measured fluorescence quenching of absorption matched R6G solution in the presence of polymer before and after dialysis at pH 7.4 and 4.2 (Figure 4a,b). In acidic medium (pH = 4.2), the higher fluorescence intensity of R6G can be assigned to protonation of pendent primary amine group in poly(L-Trp-HEA)-*b*-poly(PEGMA) which disallows PET.[44] At pH 7.4, an additional quenching (~20%) of R6G emission was observed in the dialyzed solution. This additional quenching of emission intensity, as discussed before, is attributed to the confinement effect of R6G dye molecules that further ascertain the formation of vesicular assemblies. Subsequently, on decreasing the solution pH of the above R6G encapsulated dialyzed vesicular solution from 7.4 to 4.2, the fluorescence intensity of the resulting solution increased by ~1.8 times and became close to that of polymer-free solution at pH 7.4, as shown in Figure 4c. The above observation clearly suggests the release of the encapsulated hydrophilic guest molecules (R6G) from the confined water pool inside the vesicle to bulk water on decreasing the solution pH from 7.4 to 4.2. As shown in the previous page, the CAC measurement also revealed the capability of the poly(L-Trp-HEA)-*b*-poly(PEGMA) copolymer to encapsulate Nile Red, a hydrophobic dye, at pH 7.4 and 4.2. As shown in Figure 2, the block copolymer containing Nile Red showed an emission maximum at 616 nm at pH 7.4 with substantial increase in the emission intensity compared to its polymer-free aqueous solution of same pH, which clearly indicated the encapsulation of Nile Red in the hydrophobic bilayer region of the vesicles. On decreasing the pH of the above Nile Red encapsulated vesicular solution from 7.4 to 4.2, a red-shift of 5 nm (616 to 621 nm) in the emission maxima was observed without any significant change in the intensity. This indicated that Nile Red was still located in a hydrophobic

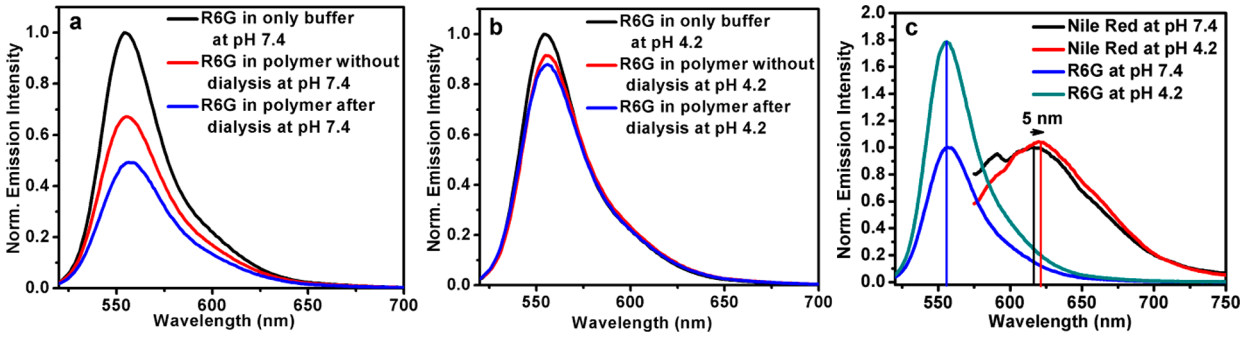

Figure 4. Fluorescence quenching of absorption matched R6G solution in the presence of polymer with and without dialysis at two representative solution pH: (a) 7.4 and (b) 4.2. (c) Intensity normalized emission spectra of Nile Red and R6G encapsulated in 0.2 mM poly(L-Trp-HEA)-*b*-poly(PEGMA) solution at two representative solution pH: 7.4 and 4.2.

DOI: 10.1021/la504165e
Langmuir 2015, 31, 32−41

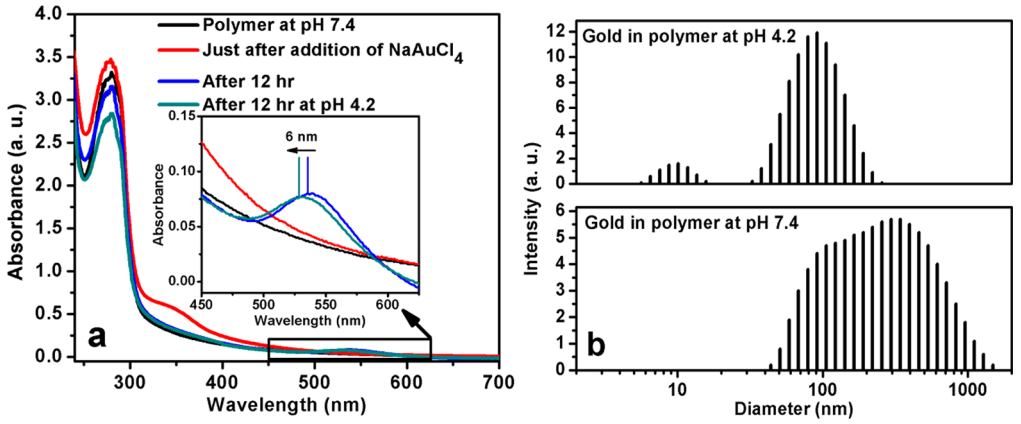

Figure 5. (a) UV−vis absorption spectra of 0.02 mM aqueous polymer solution at pH 7.4 at different time interval to follow the synthesis of AuNPs. Also, after synthesis of AuNPs (12 h) at pH 7.4 the pH of the solution was adjusted to 4.2 by adding 1 M HCl, and the spectra were recorded. (b) Size distribution profile of the polymer−AuNPs composite obtained from dynamic light scattering measurement at two representative solution pH: 7.4 and 4.2.

environment, i.e., inside the core of the micelles, even at lower solution pH but in the lower pH Nile Red experienced relatively less hydrophobic environment (Figure 4c). To rationalize the pH-induced vesicle to micelle transition of poly(L-Trp-HEA)-*b*-poly(PEGMA), we propose that at pH 7.4 the amino groups of the tryptophan were free/deprotonated, making the poly(L-Trp-HEA) block quite hydrophobic which provided the right hydrophobic/hydrophilic balance to form vesicles. Below the transition pH the amino groups became protonated which decreased the hydrophobicity of the poly(L-Trp-HEA) block. However, the pendant indole segments remained deprotonated, and consequently the poly(L-Trp-HEA) remained sufficiently hydrophobic to provide the right hydrophobic/hydrophilic balance to form micellar aggregates. As the vesicular bilayer was formed by more hydrophobic deprotonated poly(L-Trp-HEA) blocks, it is expected that the packing of the chains would be significantly higher than the corresponding micellar cores formed by the less hydrophobic blocks. This explains the observed lower value of the thickness of vesicle bilayer than the corresponding micelle diameter.

Gold Nanoparticle Decorated Vesicle Preparation. Utility of such poly(L-Trp-HEA)-*b*-poly(PEGMA) copolymer that spontaneously form vesicles at pH 7.4 is worth exploring. In this respect, we first attempted to prepare AuNPs via *in situ* reduction of $HAuCl_4$ using the present polymer. Sastry et al.[45] have shown that tryptophan is capable of forming and stabilizing AuNPs, where the indole group of tryptophan is the reducing segment and the amine group is primarily involved in the complexation with the gold surface. On the other hand, poly(ethylene glycol) is also known to reduce $HAuCl_4$ to form AuNPs;[17,46] e.g., Chen et al. proved that aggregation of PEG-based block copolymers and hydrophobicity of the aggregates play a very important role in the stabilization of the gold particles.[47] In the present work, we first allowed vesicle formation to occur by dissolving poly(L-Trp-HEA)-*b*-poly(PEGMA) at pH 7.4, and then the resulting solution was mixed with the $NaAuCl_4$ solution in a 10:1 molar ratio of L-Trp-HEA units:$NaAuCl_4$. The solutions were stirred at 450 rpm overnight. After mixing $NaAuCl_4$ solution, the solution immediately turned light yellow, which gradually changed to red pink which indicated formation of AuNPs in solution. The reduction process was monitored by UV−vis absorption spectroscopy, which is shown in Figure 5a. Figure 5a reveals that the block copolymer vesicular solution gave only absorption peak at 280 nm due to presence of tryptophan moiety in the polymer chain. An additional broad peak at 320−340 nm appeared just after addition of $NaAuCl_4$ solution due to formation of ligand to metal charge transfer (LMCT) complex that disappeared after complete reduction of Au^{3+} salt. A new peak was visible at 535 nm due to the surface plasmon resonance of AuNPs.[48,49] After synthesis of AuNPs at pH 7.4 we have adjusted the solution pH to 4.2 by adding the required amount of 1 M HCl, and the UV−vis spectra was recorded, which show a plasmon resonance peak at 529 nm, i.e., 6 nm blue-shift in comparison to the starting AuNP solution (at pH 7.4). The 6 nm blue-shift in the absorption maximum reflects that the AuNPs were in a better dispersed state in comparison to pH 7.4. The intensity of absorption of polymer−AuNPs composite solution at pH 4.2 was nearly the same as at pH 7.4, suggesting that no precipitation of the AuNPs took place due to change in pH of the solution. A slight decrease in the intensity of absorption compared to the original composite solution at a pH of 7.4 was due to a dilution effect because of pH adjustment.

We have also investigated the effect of pH on the polymer−AuNPs composite by DLS and TEM measurements. DLS analysis (Figure 5b) showed that the average size of the gold decorated vesicles was 321 nm at pH 7.4. A slight increase in size is attributed to the increased hydrophobicity of poly(L-Trp-HEA) block due to attachment of the AuNPs.[2] At the acidic pH of 4.2, the DLS histogram showed a dual intensity-size distribution which indicated the presence of some free AuNPs in solution of size about 10 nm in addition to large gold-embedded micelles with average hydrodynamic diameter of about 100 nm. The particle size and morphology of the polymer−AuNPs composites at the two pH were also investigated by TEM (see Figure 6). The result obtained from DLS measurements corroborate well with TEM study. TEM analysis showed that the size of the AuNPs was ∼2 to 5 nm. The bilayer thickness obtained from TEM images is about 65 nm for the gold embedded vesicles, whereas in the absence of gold it is ∼40 ± 5 nm. This increase in size of vesicles is attributed to the increased hydrophobicity of poly(L-Trp-HEA) block due to attachment of AuNPs and the presence of some AuNPs that may be distributed within the PEGMA polymer chains. Du et al. reported a similar observation where the

DOI: 10.1021/la504165e
Langmuir 2015, 31, 32−41

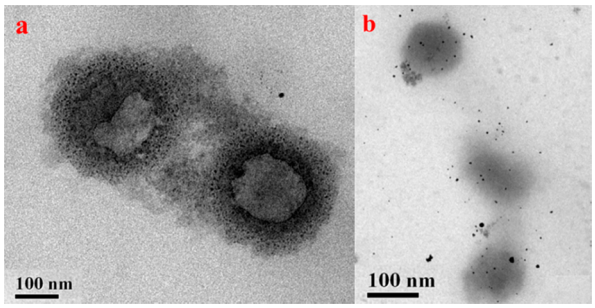

Figure 6. (a) TEM image of the AuNPs decorated vesicles obtained at 7.4 solution pH. (b) TEM image after decreasing solution pH from 7.4 to 4.2.

stained vesicles became significantly larger than the precursor vesicles after the *in situ* synthesis of the AuNPs, and this procedure was undertaken to selectively stain the walls of the vesicles.[2,7] At pH ∼ 4.2, we observed the formation of micelle by poly(L-Trp-HEA)-*b*-poly(PEGMA) copolymer in which spherical AuNPs are in a well-dispersed state, present both as embedded to micelles and as free nanoparticles in bulk water. This pH-induced organization of the AuNPs into the polymer nanostructures could be explained by changes in the local environment.

At pH 4.2 all of the amine groups of poly(L-Trp-HEA) block are in a fully protonated state, and the electrostatic repulsion between the positively charged results in the increased dispersion of the AuNPs. On the other hand, at physiological pH (7.4), the produced AuNPs were readily stabilized by the complexation with free primary amine groups (deprotonated) of tryptophan units. Additionally, some AuNPs may be distributed within the hydrophilic PEGMA polymer chains present close to the hydrophobic bilayer region of the vesicles. This explains why the gold nanoparticles were concentrated around the vesicular bilayer and less/almost no distribution of AuNPs into the water-filled central portion of vesicles. The above observation is in agreement with the previous literature reports.[7,50,51] In addition, more hydrophobicity of the vesicular shell than that of the micellar core may also favor better attachment of the AuNPs to vesicular hydrophobic shell compared to the micellar core. In our previous study we had observed similar hydrophobicity driven AuNPs dispersion in block/random copolymer−AOT systems.[17]

To investigate the surface charge of polymer nanostructures and gold-decorated polymer aggregates at different solution pH, we have performed zeta potential measurements. Aqueous solution of poly(L-Trp-HEA)-*b*-poly(PEGMA) copolymer (0.2 mM) showed zeta potential of −0.2 and 16.7 mV at pH 7.4 and pH 4.2, respectively, as expected from its deprotonated and protonated forms, respectively. After *in situ* incorporation of AuNPs into polymer nanostructures, polymer−AuNPs composite solutions showed zeta potential of −1.1 and 14.3 mV at pH 7.4 and 4.2, respectively. This experiment clearly revealed that in acidic pH (4.2) both the block copolymer and polymer−AuNPs composite solution showed sufficiently surface positive charge. This supports our explanation of the pH-dependent nanostructure formation. It should be noted that the molar ratio of the poly(L-Trp-HEA) and $NaAuCl_4$ in our experiment was kept at 10:1 for the *in situ* formation of the AuNPs-decorated vesicles. When the ratio was lowered to 5:1, the increase in the hydrophobicity of the poly(L-Trp-HEA) block resulted in precipitation within 7 days, while the former solution showed long-term stability in aqueous media up to 60 days. Hence, this method of formation of the AuNPs-decorated vesicles is quite attractive since it allows for *in situ* formation of AuNPs followed by formation of gold-embedded vesicles (polymersomes).

Study of Energy Transfer between AuNPs and R6G Dye (NSET) in Polymer Nanostructures. The energy transfer process between donor and acceptor is strongly dependent on the distance between them; hence, successful application of energy transfer processes requires precise control over their relative position. In this respect nanostructures of poly(L-Trp-HEA)-*b*-poly(PEGMA) copolymer were very useful because they provided opportunities for precise positioning of the donor and acceptor. Herein, we investigated nanometal surface energy transfer (NSET) from R6G dye (as a donor) to AuNPs (as an acceptor) embedded in nanostructures formed by the self-assembly of poly(L-Trp-HEA)-*b*-poly(PEGMA). The purpose of using AuNPs as an acceptor and hydrophilic guest molecules (R6G) as a donor in poly(L-Trp-HEA)-*b*-poly(PEGMA) copolymer nanostructures at pH 7.4 and 4.2 is to get a better understanding about how the energy transfer efficiency varies as a result of altered accessibility of the dye

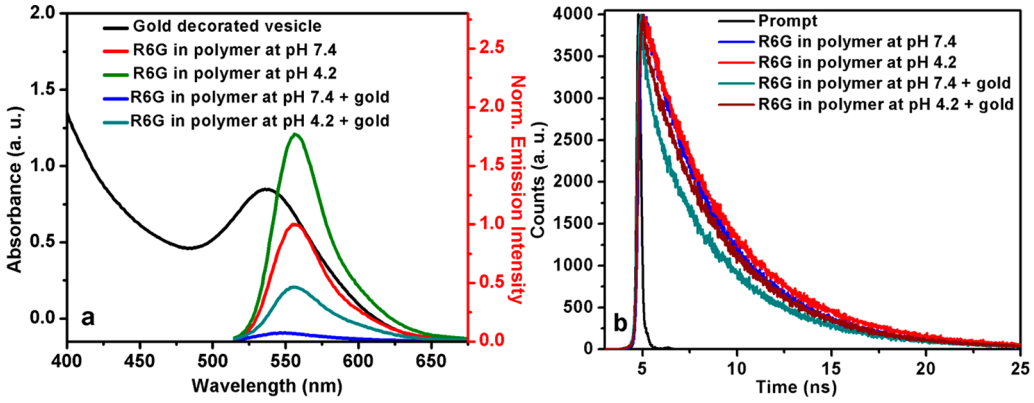

Figure 7. (a) Absorption spectra of AuNPs confined in the poly(L-Trp-HEA)-*b*-poly(PEGMA) vesicles along with normalized fluorescence spectra of the donor (R6G) in poly(L-Trp-HEA)-*b*-poly(PEGMA) copolymer nanostructures (λ_{ex} = 480 nm) at two representative pH (7.4 and 4.2) in the presence and absence of AuNPs (acceptor) which are synthesized *in situ* by the vesicular solution are also shown. (b) Time-resolved fluorescence decay of donor (R6G) corresponding to the above-mentioned solution.

DOI: 10.1021/la504165e
Langmuir 2015, 31, 32−41

molecules toward the quencher metal nanoparticles during the pH-induced structural transition like vesicle to micelle. At pH 7.4, poly(L-Trp-HEA)-*b*-poly(PEGMA) copolymer form vesicle, and therefore it was possible to encapsulate hydrophilic guest molecules (R6G) into the confined water pool inside the vesicle. Subsequently, upon lowering solution pH, poly(L-Trp-HEA)-*b*-poly(PEGMA) copolymer undergoes vesicle to micelle transition which leads to release of the encapsulated hydrophilic guest molecules (R6G) from the confined water pool inside the vesicle to the bulk water.

The absorption spectra of the AuNPs confined in the vesicles, and the steady-state fluorescence emission spectra of R6G encapsulated in poly(L-Trp-HEA)-*b*-poly(PEGMA) nanostructures, in the presence and absence of AuNPs, were recorded at the two pH levels, i.e., 7.4 and 4.2 (Figure 7a). A good spectral overlap between the fluorescence spectra of the R6G dye and the localized surface plasmon resonance (LSPR) band of the AuNPs fulfilled the criteria for the energy transfer from dye to AuNPs.[52,53] For the energy transfer study, R6G was encapsulated in the vesicular solution at pH 7.4, dialyzed, and then used for the *in situ* synthesis of AuNPs which got embedded mostly into the bilayer region of vesicles. Lower values (93% at pH 7.4 and 74% at pH 4.2) of fluorescence intensities in the presence of AuNPs, as compared to similar systems in the absence of AuNPs, support the involvement of NSET process (Figure 7a).

After getting some useful information using steady-state measurements, we performed time-resolved analysis with a picosecond setup which provided further confirmatory results about the energy transfer process. In time-resolved measurements, the energy transfer processes was monitored by decrease of the donor (R6G) lifetime in the presence of AuNPs (Figure 7b). The fluorescence lifetime of R6G was measured at the emission wavelength of 557 nm, that is, at the emission maxima. In presence of AuNPs, the donor (R6G) lifetime decreased, as shown in Table 1. Multiexponential fluorescence

Table 1. Decay Parameters for R6G−Au Systems in Confined Environment of Poly(L-Trp-HEA)-*b*-poly(PEGMA) Copolymer Nanostructures[a]

systems	solution pH	τ_1 (ns)	α_1	τ_2 (ns)	α_2	$\langle\tau\rangle$
R6G in polymer	7.4	2.03	0.17	4.37	0.83	3.97
R6G in polymer	4.2	2.71	0.24	4.96	0.76	4.42
R6G in polymer + AuNPs	7.4	0.86	0.57	3.22	0.43	1.87
R6G in polymer + AuNPs	4.2	1.25	0.31	3.81	0.69	3.02

[a]Error is ±10% in all TCSPC result.

decay was determined by using the equation $\langle\tau\rangle = \tau_1\alpha_1 + \tau_2\alpha_2$, where τ_1 and τ_2 are the lifetime components, with α_1 and α_2 being their corresponding relative weights. In the present case, we have used the average lifetime quenching data to determine the energy transfer efficiency. NSET parameters for R6G−Au systems in confined environment of poly(L-Trp-HEA)-*b*-poly(PEGMA) copolymer nanostructures at the two pH are listed in Table 2. It can be inferred from the data presented in Table 2, which on changing the pH from 7.4 to 4.2 the efficiency of energy transfer decreased from 53% to 32% whereas the calculated average distance between the donor (R6G) and the acceptor (AuNPs) increased from 66.7 to 92.2 Å, which allowed us to monitor the vesicle-to-micelle transition

Table 2. Nanometal Surface Energy Transfer (NSET) Parameters for R6G−Au Systems in Confined Environment of Poly(L-Trp-HEA)-*b*-poly(PEGMA) Copolymer Nanostructures

systems	solution pH	λ_{ex} (nm)	Φ_{sample}	E^a (%)	E^b (%)	d_0 (Å)	d^b (Å)
R6G in polymer	7.4	480	0.48				
R6G in polymer	4.2	480	0.73				
R6G in polymer + AuNPs	7.4	480	0.48	93.0	53.0	68.7	66.7
R6G in polymer + AuNPs	4.2	480	0.73	74.0	32.0	76.3	92.2

[a]From steady-state measurement. [b]From time-resolved measurement.

by NSET process. When vesicles were transitioned to micelles *in situ* by a stimulus like pH, the NSET molecules were released and diffused apart, reducing the energy transfer. By monitoring the NSET efficiency, release of the core-loaded probes to biological media can potentially be demonstrated. Energy transfer based stimuli-responsive nanocarriers for drug delivery are used to monitor the stimuli-responsive dynamic release of drugs in the biological system.[26,54]

SUMMARY

We have demonstrated the synthesis of a PEG containing block copolymer synthesized via RAFT polymerization technique and studied its pH-dependent self-assembly behavior to form nanostructured aggregates in aqueous solution. We showed that the block copolymer was capable of reversible morphological transitions in aqueous solution on changing the pH of the solution, with vesicle formation happening at physiological pH and micelle formation at acidic pH. The pH-dependent nanostructural changes were attributed to the hydrophobicity of the poly(L-Trp-HEA) block due to protonation and deprotonation of the α-amino group at acidic and physiological pH, respectively. The polymer vesicles could be utilized to reduce $HAuCl_4$ and stabilize the resulting AuNPs by embedding in the hydrophobic shell of the vesicles. A hydrophilic dye, R6G, was loaded in the hydrophilic core of the vesicles, resulting in Au-R6G NSET pair with high efficiency of energy transfer. The efficiency of the energy transfer process decreased on transition from the vesicular to micellar form owing to the release of the R6G molecules from the vesicular core to the bulk water that enhanced the donor−acceptor distance. Hence, the present pH-responsive poly(L-Trp-HEA)-*b*-poly(PEGMA) copolymer nanostructures could provide a suitable scaffold for the NSET process, and such well-defined stable confined hybrid spherical assemblies with efficient loading of the fluorescent guest molecules and AuNPs will certainly be helpful to further explore its potential applicability in sensing and medicinal chemistry.

ASSOCIATED CONTENT

Supporting Information

Additional fluorescence quenching data, NMR spectra of the block copolymers, procedures for synthesis of tryptophan containing monomer (Boc-L-Trp-HEA) and poly(PEGMA)-based macro-chain transfer agent (CTA); instruments and methods used for recording NMR spectra, GPC, UV−vis, steady-state and time-resolved fluorescence spectra, measuring

DOI: 10.1021/la504165e
Langmuir 2015, 31, 32−41

turbidity, structural characterization (TEM, DLS), determination of critical aggregation concentration (CAC), encapsulation of Rhodamine 6G (R6G) in the vesicular assemblies, calculation of fluorescence quantum yield, NSET parameters. This material is available free of charge via the Internet at http://pubs.acs.org.

AUTHOR INFORMATION

Corresponding Author

*E-mail dibakar@chem.iitkgp.ernet.in, dibakar@live.in; Ph +91-3222-282326; Fax +91-3222-282252 (D.D.).

Notes

The authors declare no competing financial interest.

ACKNOWLEDGMENTS

Financial support from SRIC, Indian Institute of Technology Kharagpur (project code NPA with institute approval numbers IIT/SRIC/CHY/NPA/2014-15/81) is acknowledged. Authors are also thankful to Prof. N. Sarkar for providing some laboratory facilities. C.M. and R.B. acknowledge UGC, New Delhi, and S.M. acknowledges CSIR, New Delhi, for Senior Research Fellowships.

REFERENCES

(1) Du, J.; O'Reilly, R. K. Advances and Challenges in Smart and Functional Polymer Vesicles. *Soft Matter* **2009**, *5*, 3544−3561.
(2) Li, Y.; Smith, A. E.; Lokitz, B. S.; McCormick, C. L. In Situ Formation of Gold-"Decorated" Vesicles from a RAFT-Synthesized, Thermally Responsive Block Copolymer. *Macromolecules* **2007**, *40*, 8524−8526.
(3) Charleux, B.; Delaittre, G.; Rieger, J.; D'Agosto, F. Polymerization-Induced Self-Assembly: From Soluble Macromolecules to Block Copolymer Nano-Objects in One Step. *Macromolecules* **2012**, *45*, 6753−6765.
(4) Hu, J.; Liu, S. Responsive Polymers for Detection and Sensing Applications: Current Status and Future Developments. *Macromolecules* **2010**, *43*, 8315−8330.
(5) Chen, T.; Yang, M. X.; Wang, X. J.; Tan, L. H.; Chen, H. Y. Controlled Assembly of Eccentrically Encapsulated Gold Nanoparticles. *J. Am. Chem. Soc.* **2008**, *130*, 11858−11859.
(6) Azzam, T.; Eisenberg, A. Monolayer-Protected Gold Nanoparticles by the Self-assembly of Micellar Poly(ethylene oxide)-*b*-Poly(ε-caprolactone) Block Copolymer. *Langmuir* **2007**, *23*, 2126−2132.
(7) Du, J. Z.; Tang, Y. Q.; Lewis, A. L.; Armes, S. P. pH-Sensitive Vesicles Based on a Biocompatible Zwitterionic Diblock Copolymer. *J. Am. Chem. Soc.* **2005**, *127*, 17982−17983.
(8) Banerjee, R.; Dhara, D. Functional Group-Dependent Self-Assembled Nanostructures from Thermo-Responsive Triblock Copolymers. *Langmuir* **2014**, *30*, 4137−4146.
(9) Esser-Kahn, A. P.; Odom, S. A.; Sottos, N. R.; White, S. R.; Moore, J. S. Triggered Release from Polymer Capsules. *Macromolecules* **2011**, *44*, 5539−5553.
(10) Maiti, C.; Dey, D.; Mandal, S.; Dhara, D. Thermoregulated Formation and Disintegration of Cationic Block Copolymer Vesicles: Fluorescence Resonance Energy Transfer Study. *J. Phys. Chem. B* **2014**, *118*, 2274−2283.
(11) Lokitz, B. S.; Convertine, A. J.; Ezell, R. G.; Heidenreich, A.; Li, Y.; McCormick, C. L. Responsive Nanoassemblies via Interpolyelectrolyte Complexation of Amphiphilic Block Copolymer Micelles. *Macromolecules* **2006**, *39*, 8594−8602.
(12) Discher, B. M.; Won, Y.-Y.; Ege, D. S.; Lee, J. C.-M.; Bates, F. S.; Discher, D. E.; Hammer, D. A. Polymersomes: Tough Vesicles Made from Diblock Copolymers. *Science* **1999**, *284*, 1143−1146.
(13) Wu, J.; Eisenberg, A. Proton Diffusion across Membranes of Vesicles of Poly(styrene-b-acrylic Acid) Diblock Copolymers. *J. Am. Chem. Soc.* **2006**, *128*, 2880−2884.
(14) Soo, P. L.; Eisenberg, A. Preparation of Block Copolymer Vesicles in Solution. *J. Polym. Sci., Part B* **2004**, *42*, 923−938.
(15) Antonietti, M.; Förster, S. Vesicles and Liposomes: A Self-Assembly Principle Beyond Lipids. *Adv. Mater.* **2003**, *15*, 1323−1333.
(16) Dan, K.; Ghosh, S. One-Pot Synthesis of an Acid-Labile Amphiphilic Triblock Copolymer and its pH-Responsive Vesicular Assembly. *Angew. Chem., Int. Ed.* **2013**, *52*, 7300−7305.
(17) Banerjee, R.; Dutta, S.; Pal, S.; Dhara, D. Spontaneous Formation of Vesicles by Self-Assembly of Cationic Block Copolymer in the Presence of Anionic Surfactants and Their Application in Formation of Polymer Embedded Gold Nanoparticles. *J. Phys. Chem. B* **2013**, *117*, 3624−3633.
(18) Cai, Y.; Aubrecht, K. B.; Grubbs, R. B. Thermally Induced Changes in Amphiphilicity Drive Reversible Restructuring of Assemblies of ABC Triblock Copolymers with Statistical Polyether Blocks. *J. Am. Chem. Soc.* **2011**, *133*, 1058−1065.
(19) Sundararaman, A.; Stephan, T.; Grubbs, R. B. Reversible Restructuring of Aqueous Block Copolymer Assemblies through Stimulus-Induced Changes in Amphiphilicity. *J. Am. Chem. Soc.* **2008**, *130*, 12264−12265.
(20) Moughton, A. O.; O'Reilly, R. K. Thermally Induced Micelle to Vesicle Morphology Transition for a Charged Chain End Diblock Copolymer. *Chem. Commun.* **2010**, *46*, 1091−1093.
(21) Sperling, R. A.; Gil, P. R.; Zang, F.; Zanella, M.; Parak, W. J. Biological Applications of Gold Nanoparticles. *Chem. Soc. Rev.* **2008**, *37*, 1896−1908.
(22) Kim, D.; Jeong, Y. Y.; Jon, S. A Drug-Loaded Aptamer-Gold Nanoparticle Bioconjugate for Combined CT Imaging and Therapy of Prostate Cancer. *ACS Nano* **2010**, *4*, 3689−3696.
(23) Luo, Y.; Shiao, Y.; Huang, Y. Release of Photoactivatable Drugs from Plasmonic Nanoparticles for Targeted Cancer Therapy. *ACS Nano* **2011**, *5*, 7796−7804.
(24) Chen, Y.; O'Donoghue, M. B.; Huang, Y.; Kang, H.; Phillips, J. A.; Chen, X.; Estevez, M. C.; Yang, C. J.; Tan, W. A Surface Energy Transfer Nanoruler for Measuring Binding Site Distances on Live Cell Surfaces. *J. Am. Chem. Soc.* **2010**, *132*, 16559−16570.
(25) Raino, G.; Stoferle, T.; Park, C.; Kim, H.; Topuria, T.; Rice, P. M.; Chin, I.; Miller, R.; Mahrt, R. F. Plasmonic Nanohybrid with Ultrasmall Ag Nanoparticles and Fluorescent Dyes. *ACS Nano* **2011**, *5*, 3536−3541.
(26) Chen, H.; Kim, S.; Li, L.; Wang, S.; Park, K.; Cheng, J. X. Release of Hydrophobic Molecules from Polymer Micelles into Cell Membranes Revealed by Forster Resonance Energy Transfer Imaging. *Proc. Natl. Acad. Sci. U. S. A.* **2008**, *105*, 6596−6601.
(27) Jiwpanich, S.; Ryu, J. H.; Bickerton, S.; Thayumanavan, S. Noncovalent Encapsulation Stabilities in Supramolecular Nanoassemblies. *J. Am. Chem. Soc.* **2010**, *132*, 10683−10685.
(28) Wu, Y.; Hu, H.; Hu, J.; Liu, T.; Zhang, G.; Liu, S. Thermo- and Light-Regulated Formation and Disintegration of Double Hydrophilic Block Copolymer Assemblies with Tunable Fluorescence Emissions. *Langmuir* **2013**, *29*, 3711−3720.
(29) Lai, J. T.; Filla, D.; Shea, R. Functional Polymers from Novel Carboxyl-Terminated Trithiocarbonates as Highly Efficient RAFT Agents. *Macromolecules* **2002**, *35*, 6754−6756.
(30) Banerjee, R.; Gupta, S.; Dey, D.; Maiti, S.; Dhara, D. Synthesis of PEG Containing Cationic Block Copolymers and Their Interaction with Human Serum Albumin. *React. Funct. Polym.* **2014**, *74*, 81−89.
(31) Drachuk, I.; Shchepelina, O.; Lisunova, M.; Harbaugh, S.; Kelley-Loughnane, N.; Stone, M.; Tsukruk, V. V. pH-Responsive Layer-by-Layer Nanoshells for Direct Regulation of Cell Activity. *ACS Nano* **2012**, *6*, 4266−4278.
(32) Alexandridis, P.; Holzwarth, J. F.; Hatton, T. A. Micellization of Poly(ethylene oxide) Poly(propylene oxide)-Poly(ethy1ene oxide) Triblock Copolymers in Aqueous Solutions: Thermodynamics of Copolymer Association. *Macromolecules* **1994**, *27*, 2414−2425.

DOI: 10.1021/la504165e
Langmuir 2015, 31, 32−41

(33) Chen, C.; Liu, G.; Liu, X.; Pang, S.; Zhu, C.; Lv, L.; Ji, J. Photo-Responsive, Biocompatible Polymeric Micelles Self-Assembled from Hyperbranched Polyphosphate-Based Polymers. *Polym. Chem.* **2011**, *2*, 1389−1397.
(34) Alexandridis, P.; Holzwarth, J. F.; Hatton, T. A. Micellization of Poly(ethy1ene oxide)-Poly(propylene oxide)-Poly(ethy1ene oxide) Triblock Copolymers in Aqueous Solutions: Thermodynamics of Copolymer Association. *Macromolecules* **1994**, *27*, 2414−2425.
(35) Dan, K.; Ghosh, S. pH-Responsive Aggregation of Amphiphilic Glyco-Homopolymer. *Macromol. Rapid Commun.* **2012**, *33*, 127−132.
(36) Laskar, P.; Samanta, S.; Ghosh, S. K.; Dey, J. In Vitro Evaluation of pH-Sensitive Cholesterol-Containing Stable Polymeric Micelles for Delivery of Camptothecin. *J. Colloid Interface Sci.* **2014**, *430*, 305−314.
(37) Liu, C.; Yuan, J.; Luo, X.; Chen, M.; Chen, Z.; Zhao, Y.; Li, X. Folate-Decorated and Reduction-Sensitive Micelles Assembled from Amphiphilic Polymer-Camptothecin Conjugates for Intracellular Drug Delivery. *Mol. Pharmaceutics* **2014**, *11*, 4258−4269.
(38) Barkey, N. M.; Preihs, C.; Cornnell, H. H.; Martinez, G.; Carie, A.; Vagner, J.; Xu, L.; Lloyd, M. C.; Lynch, V. M.; Hruby, V. J.; Sessler, J. L.; Sill, K. N.; Gillies, R. J.; Morse, D. L. Development and in Vivo Quantitative Magnetic Resonance Imaging of Polymer Micelles Targeted to the Melanocortin 1 Receptor. *J. Med. Chem.* **2013**, *56*, 6330−6338.
(39) Liu, F.; Eisenberg, A. Preparation and pH Triggered Inversion of Vesicles from Poly(acrylic Acid)-*block*-Polystyrene-*block*-Poly(4-vinyl Pyridine). *J. Am. Chem. Soc.* **2003**, *125*, 15059−15064.
(40) Rao, V. G.; Mandal, S.; Ghosh, S.; Banerjee, C.; Sarkar, N. Study of Fluorescence Resonance Energy Transfer in Zwitterionic Micelle: Ionic-Liquid-Induced Changes in FRET Parameters. *J. Phys. Chem. B* **2012**, *116*, 12021−12029.
(41) Savariar, E. N.; Aathimanikandan, S. V.; Thayumanavan, S. Supramolecular Assemblies from Amphiphilic Homopolymers: Testing the Scope. *J. Am. Chem. Soc.* **2006**, *128*, 16224−16230.
(42) Mahato, P.; Saha, S.; Choudhury, S.; Das, A. Solvent-Dependent Aggregation Behavior of a New Ru(II)-Polypyridyl based Metallosurfactant. *Chem. Commun.* **2011**, *47*, 11074−11076.
(43) Vaiana, A. C.; Neuweiler, H.; Schulz, A.; Wolfrum, J.; Sauer, M.; Smith, J. C. Fluorescence Quenching of Dyes by Tryptophan: Interactions at Atomic Detail from Combination of Experiment and Computer Simulation. *J. Am. Chem. Soc.* **2003**, *125*, 14564−14572.
(44) Bojinov, V. B.; Konstantinova, T. N. Fluorescent 4-(2,2,6,6-Tetramethylpiperidin-4-ylamino)-1,8-Naphthalimide pH Chemosensor Based on Photoinduced Electron Transfer. *Sens. Actuators, B* **2007**, *123*, 869−876.
(45) Selvakannan, P. R.; Mandal, S.; Phadtare, S.; Gole, A.; Pasricha, R.; Adyanthaya, S. D.; Sastry, M. Water-dispersible Tryptophan-protected Gold Nanoparticles Prepared by the Spontaneous Reduction of Aqueous Chloroaurate Ions by the Amino Acid. *J. Colloid Interface Sci.* **2004**, *269*, 97−102.
(46) Sakai, T.; Alexandridis, P. Single-Step Synthesis and Stabilization of Metal Nanoparticles in Aqueous Pluronic Block Copolymer Solutions at Ambient Temperature. *Langmuir* **2004**, *20*, 8426−8430.
(47) Chen, S.; Guo, C.; Hu, G. H.; Wang, J.; Ma, J. H.; Liang, X. F.; Zheng, L.; Liu, H. Z. Effect of Hydrophobicity inside PEO−PPO−PEO Block Copolymer Micelles on the Stabilization of Gold Nanoparticles: Experiments. *Langmuir* **2006**, *22*, 9704−9711.
(48) Khullar, P.; Mahal, A.; Singh, V.; Banipal, T. S.; Kaur, G.; Bakshi, M. S. How PEO-PPO-PEO Triblock Polymer Micelles Control the Synthesis of Gold Nanoparticles: Temperature and Hydrophobic Effects. *Langmuir* **2010**, *26*, 11363−11371.
(49) Mandal, S.; Ghatak, C.; Rao, V. G.; Ghosh, S.; Sarkar, N. Pluronic Micellar Aggregates Loaded with Gold Nanoparticles (AuNPs) and Fluorescent Dyes: A Study of Controlled Nanometal Surface Energy Transfer. *J. Phys. Chem. C* **2012**, *116*, 5585−5597.
(50) Li, D.; He, Q.; Cui, Y.; Li, J. Fabrication of pH-Responsive Nanocomposites of Gold Nanoparticles/Poly(4-vinylpyridine). *Chem. Mater.* **2007**, *19*, 412−417.
(51) Hamner, K. L.; Maye, M. M. Thermal Aggregation Properties of Nanoparticles Modified with Temperature Sensitive Copolymers. *Langmuir* **2013**, *29*, 15217−15223.
(52) Singh, M. P.; Strouse, G. F. Involvement of the LSPR Spectral Overlap for Energy Transfer between a Dye and Au Nanoparticle. *J. Am. Chem. Soc.* **2010**, *132*, 9383−9391.
(53) Sen, T.; Patra, A. Resonance Energy Transfer from Rhodamine 6G to Gold Nanoparticles by Steady-State and Time-Resolved Spectroscopy. *J. Phys. Chem. C* **2008**, *112*, 3216−3222.
(54) Lu, J.; Owen, S. C.; Shoichet, M. S. Stability of Self-Assembled Polymeric Micelles in Serum. *Macromolecules* **2011**, *44*, 6002−6008.

DOI: 10.1021/la504165e
Langmuir 2015, 31, 32−41